2.6   Mercury

TJ McCoy, Smithsonian Institution, Washington, DC, USA
LR Nittler, Carnegie Institution of Washington, Washington, DC, USA

2.6.1   Introduction: The Importance of Mercury

Mercury has always held the distinction of being the terrestrial planet most unlike the others. Mercury is the smallest of the terrestrial planets, with a diameter a little more than a third that of Earth (and about 45% larger than that of the Moon). Its relatively high density, 5.4 g cm^{-3}, indicates a large metallic core (about 3/4 of the planet's radius) compared to its silicate mantle and crust. Further, the existence of a magnetic field requires a partially molten metallic core to the present. The surface is heavily cratered but with a variety of smooth plain deposits that could either have a volcanic or impact-melt origin. Earth-based observations suggested a surface composition low in FeO (only about 3 wt%).

The proximity of Mercury to the Sun is particularly important. In one somewhat outmoded view of how the solar system formed, Mercury was assembled in the hottest region close to the Sun so that virtually all of the iron was in the metallic state, rather than oxidized to FeO (e.g., Lewis, 1972, 1974). If correct, Mercury ought to have relatively a low content of FeO. This hypothesis also predicts that Mercury should have high concentrations of refractory elements, such as calcium, aluminum, and thorium, and low concentrations of volatile elements, such as sodium and potassium, compared to the other terrestrial planets.

Alternative hypotheses tell a much more nomadic and dramatic story of Mercury's birth. In one alternative view, wandering planetesimals that might have come from as far away as Mars or the inner asteroid belt accreted to form Mercury (Wetherill, 1994). This model predicts higher FeO and volatile elements than does the high-temperature model and similar compositions among the terrestrial planets. The accretion process might have been accompanied by a monumental impact that stripped away much of the young planet's rocky mantle, accounting for the high density of the planet (Benz et al., 1988).

On 18 March 2011, after three successful flybys of Mercury, the MESSENGER spacecraft entered orbit around Mercury.

Essential to the payload of MESSENGER are three instruments designed to measure the geochemistry of the surface – an x-ray spectrometer, a gamma-ray spectrometer, and a neutron spectrometer. Together, the data returned by these three instruments – coupled with insights about planetary structure gained from tracking the spacecraft, spectral data measured in orbit, and a new and complete view of the geology of the surface (Figure 1) – have begun to revolutionize the people's understanding of Mercury. In this chapter, pre-MESSENGER views of Mercury are reviewed first, followed by the initial results from the MESSENGER mission. The implications of these first results in constraining the origin of Mercury are then discussed, followed by a look forward to future work.

2.6.2   Pre-MESSENGER View of the Chemical Composition of Mercury

Prior to MESSENGER, little was known about the bulk chemical composition of Mercury and only three compositional features were reasonably well determined: a large metallic core, a low-FeO concentration on the surface, and the presence of volatile sodium and potassium in the exosphere and, by extension, on the surface.

The mean density of Mercury is 5.43 ± 0.01 g cm^{-3} (Anderson et al., 1987), corresponding to an uncompressed density of 5.3 (Anderson et al., 1996). The uncompressed density of Mercury is by far the largest of the terrestrial planets. Earth is the closest, with a reduced density of only 4.03 g cm^{-3}. This high density was interpreted to mean that Mercury has a large metallic Fe–Ni core and a correspondingly high bulk Fe/Si ratio.

While Mercury appears to be rich in iron, its surface was thought to be poor in FeO. Prior to MESSENGER, insights into the FeO concentration of the crust came primarily from spectral observations. Such observations are difficult to make

Figure 1 Images taken with the wide-angle camera of the Mercury Dual Imaging System on 29 September 2009 during MESSENGER's third flyby of Mercury. The image on the left approximates true color using the 480, 560, and 630 nm wavelength images. The image on the right accentuates subtle color differences relative to the global average. The double-ring basin that appears deep blue on the right is the ∼290 km diameter Rachmaninoff basin. The yellow spot nearby is centered on an irregular rimless depression thought to be a volcanic vent with the yellow material representing a pyroclastic deposit.

because of the small angular separation between Mercury and the Sun. This results in a long path through the atmosphere and concomitantly large corrections. Vilas (1988) summarized the reflectance observations. Observations in the mid-infrared were reported by Sprague et al. (1994) and in the microwave and mid-infrared by Jeanloz et al. (1995). Color observations from recalibrated Mariner 10 data were reported by Robinson and Lucey (1997). Blewett et al. (2002) and Warrell (2003) made detailed comparisons between the spectra of Mercury and that of heavily space weathered ('mature') pure anorthosite regions on the Moon. Such regions (whether mature or not) have <3 wt% FeO. Lunar anorthosite and Mercurian spectra are quite similar. This implies that most of Mercury's surface has an FeO content like that of mature lunar anorthosites, <3 wt%. This is consistent with an assessment of the FeO content of the Mercurian surface (Blewett et al., 1997) by a different spectral technique developed for the Moon by Lucey et al. (1995). This approach allows both maturity and FeO to be deduced and indicates an FeO content of about 3 wt%.

Mercury is surrounded by a tenuous exosphere that is supplied primarily by the planet's surface materials, while the region around Mercury is filled with ions that originate from interactions of the solar wind with Mercury's space environment and through ionization of its exosphere. Ground-based observations of Mercury found that the exosphere contains sodium, potassium, and calcium (Killen et al., 2007; Potter and Morgan, 1985, 1986). These elements are derived from

the surface by a variety of loss mechanisms, apparently dominated by sputtering (e.g., Killen and Ip, 1999). Although it was not possible to derive surface compositions from the exosphere composition, their presence in the exosphere suggests that the surface contains volatile sodium and potassium.

2.6.3 Pre-MESSENGER Models for the Origin of Mercury

Prior to MESSENGER, several classes of models were developed to explain the physical and chemical properties of Mercury, including (1) physical models of differential accumulation of metal and silicate or impact removal of silicates from a differentiated Mercury to account for the planet's large metallic core, (2) high-temperature evaporation or condensation in the region where Mercury was formed, (3) mixing of high-temperature ingredients with more volatile ones, and (4) formation through melting of known chondritic meteorites.

2.6.3.1 Physical Models for Metal Enrichment in Mercury

Some authors have focused on physical mechanisms to account for the high density of Mercury, searching for ways to enrich metal compared to silicate. Weidenschilling (1976) appealed to aerodynamic fractionation to separate metal from silicate as Mercury was accreting. A more dramatic model involves a giant impact stripping of the silicate mantle off Mercury after it has differentiated (Benz et al., 1988; Cameron et al., 1988; Wetherill, 1988). Both models account for the high metal/silicate ratio of Mercury, but neither explicitly predicts the FeO content of the planet. However, the impact model implies scrambling of planetesimals from a wide range of heliocentric distances (to account for the high relative velocities of impacting planetesimals). This implies that Mercury ought to have a relatively high FeO content like the other terrestrial planets, but it does not. In addition, successful impact models required extreme conditions (Benz et al., 1988): (1) The bodies contain exceptionally large (32 wt%) metal concentrations initially; (2) the collisions were either head-on at 20 km s^{-1} or oblique at implausibly high collision speeds of 35 km s^{-1}; and (3) all the silicate ejecta is removed as subcentimeter-sized particles by the Poynting–Robertson effect, otherwise silicates would reaccrete onto Mercury.

2.6.3.2 High-Temperature Evaporation and Condensation Models for Mercury

Cameron (1985) estimated that temperatures in the solar nebula could have reached 2500–3500 K at Mercury's distance from the Sun. Recent models of the solar nebula do not predict such high temperatures at 0.4 AU, but it is an interesting idea worth considering. If Mercury had formed very early, perhaps by gravitational instabilities in the gas phase, then its composition could be affected by these high temperatures. There would be two main effects. First, much of the silicate would be vaporized and lost, thereby increasing the ratio of metal to silicate. Cameron (1985) assumed that the original Mercury was about 2.25 times the mass of the present Mercury. Second, the composition of the silicate would become more refractory.

Fegley and Cameron (1987) calculated the compositions of the silicate portion of the hypothetical Mercury, using both ideal and nonideal silicate magmas, assuming it began with oxides in solar proportions. The composition that most closely matches the inferred FeO concentration is very distinctive, characterized by very low SiO_2, high MgO, and no potassium. Thorium would be greatly fractionated from uranium due to formation of volatile UO_3 gas.

Theoretical models for the solar nebula indicate a decreasing temperature with increasing distance from the Sun. If the thermal gradient were steep enough, the composition of condensates from the nebula, if at equilibrium, would vary as a function of distance and temperature (Lewis, 1972, 1974). Mercury might have accreted from high-temperature condensates. These would be composed of metallic iron and FeO-free silicates. This could explain why Mercury has a large metallic core: Fe metal condenses before magnesium silicates, so could accrete first. Taylor and Scott (2003) outlined a number of serious objections to this model, yet it served as an interesting end-member case. Goettel (1988) calculated the composition of the silicate portion of an ultrarefractory Mercury, finding a composition that would contain no FeO or volatiles and large concentrations of the refractory elements aluminum, calcium, and magnesium.

2.6.3.3 Refractory-Volatile Mixtures

The presence of FeO on Mercury and the notion that planetary accretion involved mixing throughout the inner solar system motivated models involving mixing of refractory and volatile materials. Goettel (1988) and Morgan and Anders (1980) arrived at quite similar preferred compositions. The abundances of refractory elements are modest but larger than those for the Earth (Jagoutz et al., 1979; McDonough and Sun, 1995; Taylor and McLennan, 1985). Both compositions have small amounts of sodium and potassium, as required by the presence of these elements in the Mercurian atmosphere. The Morgan and Anders composition has surprisingly high Cr_2O_3. Taylor and Scott (2003) calculated the composition of a 10% partial melt at 10 kb of the Morgan and Anders composition, estimating the amount of thorium and uranium in the magma by assuming distribution coefficients of 0.001. The calculated magmas are still low in FeO but have normal basaltic levels of aluminum, calcium, and magnesium. Sodium and potassium are enhanced compared to the assumed source rock, with chondritic Th/U and subchondritic K/Th.

2.6.3.4 Formation of Mercury from Known Chondritic Meteorites

The notion that chondrites were the building blocks of the planets has a long history, but enthusiasm for the idea has waned, largely because there is no match between any known chondrite group and the bulk Earth (Drake and Righter, 2002; Taylor, 1991). Nonetheless, several authors have examined the origin of Mercury in light of known chondrites, recognizing the potential mismatch. The recognition of a clan of meteorites rich in metal and poor in FeO spurred reconsideration of this idea. These groups (CR, CH, and CB), collectively called the CR clan, were recognized largely among Antarctic meteorites

(Grossman et al., 1988; Krot et al., 2001; Scott, 1988; Weisberg et al., 1993, 1995). The new chondrites have normal levels of refractory elements but are richer in metallic iron and poorer in volatile elements like sodium, potassium, and sulfur than other chondrites. Bencubbin-like (CB) chondrites have more metal ($\sim$80 wt%) than Mercury ($\sim$70 wt%) and comparable FeO concentrations. Taylor and Scott (2003) argued that these metal-rich chondrites might be suitable Mercury building blocks. Both the silicate portion of these meteorites as an estimate of the bulk silicate portion of Mercury and a partial melt derived from that composition are somewhat lower in FeO than the composition of Morgan and Anders (1980) but also lower in refractory elements (calcium and aluminum) and volatiles (sodium and potassium).

Enstatite chondrites have also been considered as possible analogues for Mercury (Wasson, 1988). Like the hypotheses depicting Mercury as refractory-rich, this idea has been advanced because of Mercury's location close to the Sun, where Wasson (1988) suggests enstatite chondrites were formed. Burbine et al. (2002) explored the linkage between enstatite chondrites and Mercury by examining the spectral properties of enstatite achondrites and calculating the CIPW norms and x-ray spectra of partial melts produced from enstatite chondrites (McCoy et al., 1999). These authors concluded that the Mercurian surface would contain abundant enstatite, plagioclase, and diopside, with minor ($\sim$6%) calcium and magnesium sulfides. Further, x-ray spectra would distinguish such a surface from a low-FeO anorthositic crust. However, the spectral reddening of Mercury, which was thought to require nanophase metallic iron, coupled with the absence of a 0.6 μm absorption feature observed in laboratory spectra of the calcium sulfide oldhamite suggested to these authors that the low-FeO concentrations seen in enstatite chondrites, and their derived melts were poor matches from the Mercurian surface.

2.6.4 Results from the MESSENGER Mission

Although the three MESSENGER flybys of Mercury (14 January 2008, 6 October 2008, and 29 September 2009) were too brief to yield meaningful compositional data from the x-ray and gamma-ray spectrometers, they provided important insights into the geochemistry of Mercury. Confirming ground-based observations, mid-ultraviolet to near-infrared (wavelengths of 200–1300 nm) reflectance observations of the surface during MESSENGER's first flyby of Mercury yielded an ultraviolet absorption (<280 nm) and lack of a detectable 1-μm Fe^{2+} absorption band, suggesting that the ferrous oxide (Fe^{2+}) content of silicates in an average surface material is low (less than 2–3 wt%). Observations of neutral and ionized species in the exosphere of Mercury during the flybys identified several new species and further refined the understanding of the distributions of these species. The confirmation of ground-based species identifications was supplemented by the first identification of neutral Mg in the exosphere. (McClintock et al., 2008a,b, 2009) suggested magnesium on the surface of the planet, which was expected given the FeO-poor nature of the silicates. In addition to identifying Na^+, O^+, and K^+ as ionized species in the exosphere, Zurbruchen et al. (2008) reported ionized sulfur species (S^+ and H_2S^+) and water-group ions at

abundances of ~ 67 and 20%, respectively, of the combined abundance of Na$^+$ and Mg$^+$. The presence of ionized sulfur species in the exosphere strengthened arguments from ground-based observations that the surface of Mercury contains sulfur.

There had always been some debate about whether smooth plains on Mercury are volcanic or impact products, but the balance of evidence from morphology and color measurements favored the presence of volcanic plains on Mercury (Dzurisin, 1978; Hapke et al., 1980; Keiffer and Murray, 1987; Murray, 1975; Murray et al., 1975; Rava and Hapke, 1987; Spudis and Guest, 1988; Strom, 1977). Observations of the geology of Mercury during the three flybys and early stages of the orbital mission confirmed this view while expanding the range of geologic features suggestive of a complex geochemistry of the surface. Head et al. (2008) utilized the high-resolution imaging from the first Mercury flyby to examine relationships between craters and plain units and argue for a volcanic origin for those plain units. These authors argued that the degraded state of an ~ 240 km diameter crater far from Caloris and the superposition of numerous large craters on it imply an extended interval of modification. The embayment and burial of the exterior deposits of each of these superposed craters by smooth plains suggest that more recent and sequential volcanic flooding was involved, and this is supported by the presence of flowlike scarps and ghost craters, the lack of basin ejecta sculpture, and the distance from known basins. Robinson et al. (2008) and Denevi et al. (2009) mapped the global distribution of color units, arguing that smooth plains cover approximately 40% of the surface, and evidence for the volcanic origin of large expanses of plains suggests that a substantial portion of the crust originated volcanically. Prockter et al. (2010) argued that volcanic resurfacing of the floor of the ~ 290 km diameter Rachmaninoff peak-ring impact basin may have occurred relatively recently within the history of Mercury, perhaps into the second half of solar system history. Thus, Mercury's surface has been shaped, at least in part, by volcanic processes. As will be discussed later, these volcanic flows provide insights into the geochemistry of the mantle of Mercury.

While observations of the smooth plains confirmed pre-MESSENGER arguments for a volcanic origin, flyby and early orbital observations revealed a type of volcanism previously unknown from Mercury. Head et al. (2008, 2009) and Robinson et al. (2008) observed irregular rimless depressions along the margins of Caloris. The depressions are surrounded by bright, reddish deposits that mantle or discolor the surrounding terrain and become increasingly diffused toward their margins. Head et al. (2008) argued that one of these rimless depressions, which they interpret as volcanic vents, sits atop a broad, low shield volcano. While the genesis of such a shield volcano from effusive versus explosive activity is unclear, the reddish mantling deposits are consistent with a pyroclastic origin. Prockter et al. (2010) reported a rimless depression similar in morphology and color, although larger than that reported by Head et al. (2008), in the Rachmaninoff basin. The presence of pyroclastic deposits suggests the presence of sufficient volatiles in the erupting magmas to drive this style of volcanic activity.

A second type of enigmatic rimless depression is observed in impact craters. Unlike the rimless depressions interpreted as volcanic vents, these deposits, termed 'hollows' by Blewett et al. (2011), occur in clusters at scales of tens of meters to several kilometers, occur on the tops and sides of central peak mountains, and are spectrally blue. Although the origin of the hollows is unclear, Blewett et al. (2011) argued that these deposits likely involve excavation and recent loss of volatiles through some combination of sublimation, space weathering, outgassing, or pyroclastic volcanism.
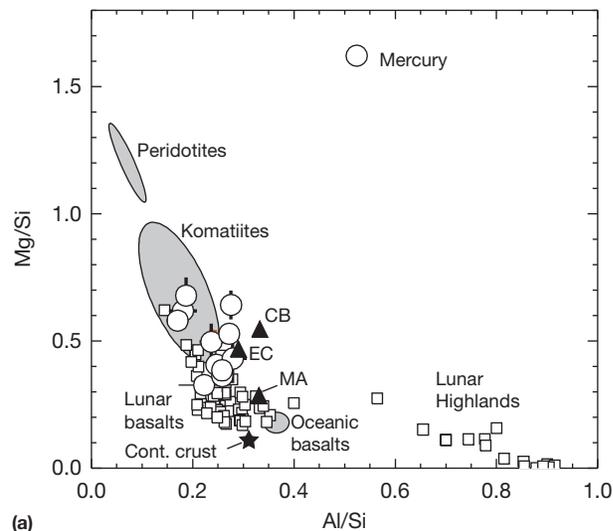
The earliest geochemical measurements of Mercury were provided by the neutron spectrometer, which indicated enrichment in equatorial regions in neutron-absorbing elements, with a measured macroscopic neutron absorption cross section similar to that of lunar basalts from Mare Crisium (Lawrence et al., 2010). Coupled with the presence of low-reflectance material (Denevi et al., 2009), it was suggested that Mercury may be enriched in iron–titanium oxides, which would darken the surface and provide an explanation for the enrichment of neutron-absorbing elements and the absence of a 1 µm absorption feature from silicates. As discussed below, these inferences proved incorrect upon orbital insertion, although the relatively high macroscopic neutron absorption cross section measurement appears robust and will require further explanation.

Upon orbital insertion, MESSENGER's x-ray and gamma-ray spectrometers began measurements of elemental abundances on Mercury, revealing both expected and surprising results. The x-ray spectrometer measurements were largely from high altitude, covering large areas primarily in the southern hemisphere (Nittler et al., 2011). As expected from both ground-based and MESSENGER observations, the surface of Mercury exhibits a high Mg/Si ratio (0.33–0.67), intermediate between terrestrial oceanic and lunar mare basalts, and highly magnesian komatiites (Figure 2). Ratios of Al/Si and Ca/Si are lower than typical terrestrial or lunar basalts. These values rule out formation and preservation of a plagioclase flotation crust, which had been suggested on to explain the exceptionally low Fe/Si ratios of 0.03–0.15 that correspond to abundances of ~ 1–4 wt% Fe if average Si concentration is ~ 25 wt%. Ti/Si ratios are exceptionally low, yielding an upper limit for Ti concentration of ~ 0.8 wt%. Taken together, the low iron and titanium abundances argue against the postulated abundant iron–titanium oxides suggested by Lawrence et al. (2010). Most surprising from the x-ray spectrometer measurements were high S/Si ratios (0.05–0.15), suggesting concentrations of the volatile element S up to ~ 4 wt% (Figure 3). The presence of significant sulfur on the surface of Mercury is consistent with the presence of ionized S$^+$ and H$_2$S$^+$ in the exosphere. Given the low iron abundances and a general correlation among Mg/Si, Ca/Si, and S/Si ratios in surface compositions, Nittler et al. (2011) suggested that the sulfur may be bound in magnesium- and/or calcium-rich sulfides, such as oldhamite or niningerite. These phases are present in highly reduced meteorites, such as enstatite chondrites.
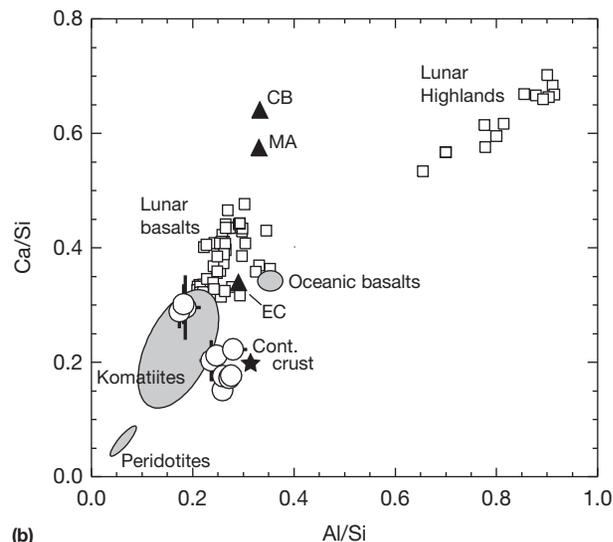
Observations from the MESSENGER gamma-ray spectrometer further argue against a volatile-depleted composition for Mercury. Peplowski et al. (2011) reported average concentrations for the moderately volatile element K (1150 ± 220 ppm) and the refractory elements Th (220 ± 60 ppb) and U (90 ± 20 ppb) for the surface of Mercury northward of $\sim 20\,^\circ$S. Mercury's K/Th ratio of 5200 ± 1800 is comparable to that of other terrestrial planets and much higher than the

value of 360 observed in the volatile-depleted lunar crust (Figure 4). The observed Th/U ratio is 2.5 ± 0.9.

Although the geochemical instrument suite on Mercury analyzed only the surface, it also provides critical insights into the interior composition of the planet. Lava flows can be used as probes of a planet's interior, assuming that they have not fractionated dramatically as they migrated to the surface. It turns out that FeO is not greatly fractionated during partial melting and modest fractional crystallization, though the Fe/Mg ratio varies dramatically because of magnesium fractionation. Robinson and Taylor (2001) showed that the ratio of FeO concentrations of terrestrial mid-ocean ridge basalts to those of the primitive terrestrial mantle is ~1.3. Thus, the FeO concentration of a lava is only about 30% higher than

the concentration of its mantle source region. This led Robinson and Taylor (2001) to conclude that Mercury contained 2–3 wt% FeO in its silicate mantle. The results from the MESSENGER mission support this conclusion, given the evidence for widespread, low-FeO volcanic plains on the surface of Mercury. These authors argued for a gradation in FeO with heliocentric distance, with Mercury lowest (2–3 wt%), Earth
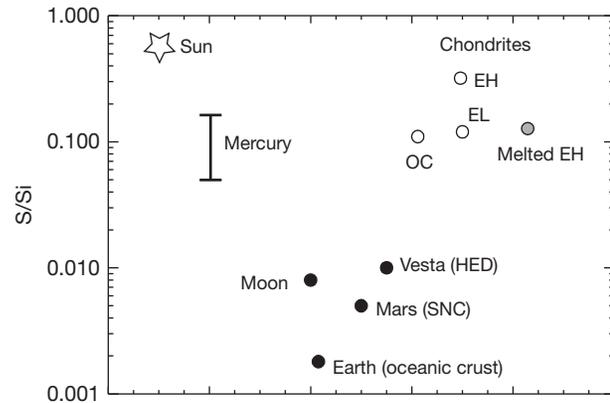

Figure 3 Sulfur to silicon ratios observed in solar system bodies. Mercury has a S/Si ratio (Nittler et al., 2011) comparable to those of ordinary chondrite (OC) and enstatite chondrite (EH, EL) meteorites and a partially melted EH chondrite (Burbine et al., 2002; McCoy et al., 1999) and much higher than those of igneous rocks in the Earth, Moon, Mars (based on the shergottite, chassignite, and nakhlite group of Martian meteorites), and Vesta (based on the howardite, eucrite, and diogenite groups of meteorites). Compositions from Lodders and Fegley (1998).
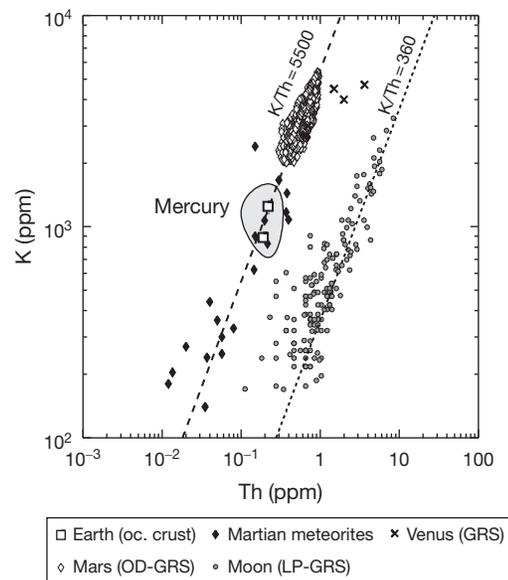

Figure 2 Mg/Si, Al/Si, and Ca/Si ratios of Mercury (open circles) from MESSENGER XRS data (Nittler et al., 2011) compared to terrestrial and lunar compositions and model predictions. Lunar and terrestrial compositions from Lodders and Fegley (1998). Filled triangles are predicted compositions of partial melts of CB chondrites (Taylor and Scott, 2003), enstatite chondrite (EC, Burbine et al., 2002; McCoy et al., 1999), and a mix of refractory and volatile materials (MA, Morgan and Anders, 1980).

Figure 4 K and Th concentrations on the Mercury surface measured by MESSENGER's gamma-ray spectrometer (2σ uncertainty, Peplowski et al., 2011) compared to those in other terrestrial planets. OD-GRS: Mars Odyssey gamma-ray spectrometer (Taylor et al., 2006a,b); LP-GRS: Lunar Prospector gamma-ray spectrometer (Prettyman et al., 2006), Venus: Soviet Venus landers. Data for Martian meteorites and terrestrial oceanic crust are from Lodders and Fegley (1998).

and Venus intermediate (about 8 wt%), and Mars and Vesta highest (18–20 wt%).

Constraints on the internal structure of have been derived from measurements of the libration (the oscillation of orbiting bodies relative to one another) (Margot et al., 2007) and, more recently, from combining the MESSENGER-derived low-degree gravity field with planetary spin parameters to yield the moment of inertia and a ratio of the moment of inertia of the solid outer shell to that of the planet (Smith et al., 2012). Observations of the amplitude of the 88-day physical libration in longitude indicate that the mantle of Mercury is decoupled from a core that is at least partially molten (Margot et al., 2007). Smith et al. (2012) utilized moment of inertia parameters in a Monte Carlo simulation of internal structures constrained by the mean radius (2440 km) and bulk density (5430 kg m^{-3}). The authors argued that the radius of the liquid outer core is 2030 km, suggesting a solid outer shell of $\sim$410 km. This outer shell is suggested to have an unusually high bulk density of 3650 kg m^{-3}. This bulk density is particularly surprising given the iron-poor nature of Mercury's surface. These authors suggest that an Fe–Si–S core could produce an immiscible, buoyant FeS melt that could solidify to form a solid FeS layer underplating the silicate crust and mantle, further reducing the thickness of that layer. If present, this would suggest a core rich in sulfur and silicon, consistent with suggestions that Mercury formed from materials formed under highly reducing conditions (see Section 2.6.5).

2.6.5   Evaluating Models for the Origin of Mercury

The pre-MESSENGER inference (Lewis, 1972, 1974; Taylor and Scott, 2003) that Mercury may have formed at highly reducing conditions (e.g., 5 log units below the iron–wüstite buffer) seems largely supported by the results from the MESSENGER mission. The low-FeO concentration in the crust implied low-FeO concentration of the mantle, apparent efficient partitioning of iron into the core, and the possible occurrence of calcium and/or magnesium sulfides inferred from x-ray spectrometer data are all consistent with reducing conditions. In contrast, the inference that Mercury would be volatile-depleted and refractory-enriched has been soundly refuted by the results from MESSENGER. Direct evidence for a relatively volatile-rich planet comes from sulfur and potassium abundances measured on the surface and from the presence of neutral and ionized sodium, potassium, and sulfur species in the exosphere. Indirect evidence for volatile-rich compositions include the suggestion of volcanic vents with associated mantling pyroclastic deposits, hollows inferred to form by excavation and recent volatile loss, and an inferred interior structure including an iron sulfide layer underplating the solid silicate shell of Mercury.

Not surprisingly, none of the physical and chemical models suggested prior to the MESSENGER mission adequately explains the full range of data and findings. However, some of the models are precluded by these data. Notably, models that require extreme heating of the planet or its precursor materials are inconsistent with the available data. Impact stripping of the silicate shell to explain the unusually large core size of Mercury would have produced significant heating and

devolatilization, particularly in collisions necessary to prevent reaccretion of the ejected material (Benz et al., 2007). Preferential vaporization of the outer silicate shell should have produced a volatile-depleted composition and, notably, a highly fractionated Th/U ratio owing to the formation of volatile UO_3, in contrast to the observed Th/U ratio of $\sim$2.5. Likewise, high-temperature nebular condensation of the precursors of Mercury should have produced materials high in the refractory elements calcium and aluminum and low in the volatiles sodium and potassium, counter to orbital observations of Mercury's surface.

Classes of models suggesting refractory-volatile mixtures, including melting of known chondritic meteorites, more closely match the observations. Melting of metal-rich Bencubbin-like meteorites and theoretical refractory-volatile mixtures produce Al/Si and Mg/Si ratios that are reasonably close to those observed on the surface of Mercury (Figure 2). However, both of these produce Ca/Si ratios significantly higher than observed (Figure 2), and volatile-depleted Bencubbin-like meteorites also produce partial melts relatively poor in sodium, potassium, and sulfur. Melting of enstatite chondrites produces Mg/Si, Al/Si, and Ca/Si ratios in the melts that are reasonably similar to the observations, although not a perfect match. Melting of enstatite chondrites also produces high sulfur in the melts, as substantial sulfur is incorporated into silicate melts under highly reducing conditions. However, melting of enstatite chondrites produces Fe/Si ratios significantly below those observed. Further, the metal abundance in enstatite chondrites is significantly below that inferred from bulk Mercury. Although Mercury likely derived from a chondritic precursor that was metal-rich with both refractory and volatile components, it seems likely that this material was either not preserved to the present and/or is not sampled among known chondritic meteorites.

2.6.6   The Future for the Exploration of Mercury

The continuing mission of MESSENGER, the European Space Agency's BepiColombo mission (Benkhoff et al., 2010), and future exploration of Mercury have many unanswered questions to address. Major geochemical drivers of MESSENGER's extended mission are understanding heterogeneity and exploring the polar regions. Results to date include limited spatially resolved x-ray spectrometer data of major and minor elements and essentially a northern hemisphere averaged gamma-ray spectrometer measurement of potassium, thorium, and uranium. Higher resolution data, particularly when coupled with a detailed knowledge of geologic and color features, can greatly elucidate the nature and origin of terrains on Mercury. While lateral heterogeneities are most easily addressed, vertical heterogeneities are equally important. A first-order question is whether the full suite of volatile elements observed on the surface of Mercury is a component of crustal rocks or surficial deposits resulting from, for example, volcanic exhalations associated with more recent pyroclastic volcanism. Spatial associations of volatile-rich compositions with pyroclastic deposits could elucidate this issue.

One of the most intriguing observations of Mercury is the presence of radar-bright deposits at the Mercury's poles. These

radar-bright deposits have been generally attributed to water ice (Harmon and Slade, 1992; Slade et al., 1992), perhaps deposited from cometary impacts in permanently or nearly permanently shadowed craters on Mercury. Alternatively, Sprague et al. (1995) suggested on the basis of mid-infrared spectral observations that these deposits might be sulfur-rich. In either case, if confirmed, these radar-bright deposits might further indicate the important role of volatiles in the history of Mercury.

Following the conclusion of the MESSENGER mission, BepiColombo will explore Mercury in 2022 with a pair of capable spacecraft designed to understand the surface and magnetosphere of the planet. In addition to pursuing a range of questions posed by MESSENGER, BepiColombo will also provide novel insights into temporal changes in Mercury (Benkhoff et al., 2010).

A milestone event in understanding the origin and evolution of Mercury would be the availability of a Mercurian sample for analyses in terrestrial laboratories. While no landed missions, including an extremely challenging sample return mission, are currently planned, the possibility remains that samples of Mercury could be identified within the meteorite population. Gladman et al. (1996) calculated that 0.5% of ejecta moving with a velocity of 4 km s^{-1} would reach Earth within 23 Ma of impact. Gladman and Coffey (2009) expanded on the range of ejection velocities and times, finding that up to 5% of ejecta could reach Earth within 30 Ma at ejection velocities of 14 km s^{-1}. These calculations suggest that impacts on Mercury within the relatively recent geologic past have the potential to deliver meteorites to Earth. With new insights into the geology, mineralogy, and geochemistry of Mercury, the very real possibility exists that a meteorite from Mercury could be tentatively identified, although at a level of confidence far below that of the Moon or Mars. If a link can be forged between a meteorite and Mercury, a new era of exploration, one largely based on isotopic systematics to understand the nature and timing of the geologic evolution of Mercury, could begin.

Acknowledgments

References

Anderson JD, Columbo G, Esposito PB, Lau PB, and Trager GB (1987) The mass, gravity field and ephemeris of Mercury. *Icarus* 71: 337–349.

Anderson JD, Jurgens RF, Lau EL, Slade MA III, and Schubert G (1996) Shape and orientation of Mercury from radar ranging data. *Icarus* 124: 690–697.

Benkhoff J, van Casteren J, Hayakawa H, et al. (2010) BepiColombo – Comprehensive exploration of Mercury: Mission overview and science goals. *Planetary and Space Science* 58: 2–20.

Benz W, Anic A, Horner J, and Whitby JA (2007) The origin of Mercury. *Space Science Reviews* 132: 189–202.

Benz W, Slattery WL, and Cameron AGW (1988) Collisional stripping of Mercury's mantle. *Icarus* 74: 516–528.

Blewett DT, Chabot NL, Denevi BW, et al. (2011) Hollows on Mercury: MESSENGER evidence for geological recent volatile-related activity. *Science* 333: 1856–1859.

Blewett DT, Hawke BR, and Lucey PG (2002) Lunar pure anorthosite as a spectral analog for Mercury. *Meteoritics and Planetary Science* 37: 1245–1254.

Blewett DT, Lucey PG, Hawke BR, Ling GG, and Robinson MS (1997) A comparison of Mercurian reflectance and spectral quantities with those of the Moon. *Icarus* 129: 217–231.

Burbine TH, McCoy TJ, Nittler LR, Benedix GK, and Cloutis EA (2002) Spectra of extremely reduced assemblages: Implications for Mercury. *Meteoritics and Planetary Science* 37: 1233–1244.

Cameron AGW (1985) The partial volatilization of Mercury. *Icarus* 64: 285–294.

Cameron AGW, Fegley B Jr., Benz W, and Slatterly WL (1988) The strange density of Mercury: Theoretical considerations. In: Vilas F, Chapman CR, and Matthews MS (eds.) *Mercury*, pp. 692–708. Tucson, AZ: University of Arizona Press.

Denevi BW, Robinson MS, Solomon SC, et al. (2009) The evolution of Mercury's crust: A global perspective from MESSENGER. *Science* 324: 613–618.

Drake MJ and Righter K (2002) Determining the composition of the Earth. *Nature* 416: 39–44.

Dzurisin D (1978) The tectonic and volcanic history of Mercury as inferred from studies of scarps, ridges, troughs and other lineaments. *Journal of Geophysical Research* 83: 4883–4906.

Fegley B Jr. and Cameron AGW (1987) A vaporization model for iron/silicate fractionation in the Mercury protoplanet. *Earth and Planetary Science Letters* 82: 207–222.

Gladman B, Burns JA, Duncan M, Lee P, and Levison H (1996) The exchange of impact ejecta between planets. *Science* 298: 1752–1756.

Gladman B and Coffey J (2009) Mercurian impact ejecta: Meteorites and mantle. *Meteoritics and Planetary Science* 44: 285–291.

Goettel KA (1988) Present bounds on the bulk composition of Mercury: Implications for planetary formation processes. In: Vilas F, Chapman CR, and Matthews MS (eds.) *Mercury*, pp. 613–621. Tucson, AZ: University of Arizona Press.

Grossman JN, Rubin AE, and MacPherson GJ (1988) ALH85085: A unique volatile–poor carbonaceous chondrite with possible implications for nebular fractionation processes. *Earth and Planetary Science Letters* 91: 33–54.

Hapke B, Christman C, Rava BB, and Mosher J (1980) A color-ratio map of Mercury. In: *Proceedings of 11th Lunar and Planetary Science Conference*, pp. 817–821.

Harmon JK and Slade MA (1992) Radar mapping of Mercury: Full-disk images and polar anomalies. *Science* 258: 640–642.

Head JW, Murchie SL, Prockter LM, et al. (2008) Volcanism on Mercury: Evidence from the first MESSENGER flyby. *Science* 321: 69–72.

Head JW, Murchie SL, Prockter LM, et al. (2009) Volcanism on Mercury: Evidence from the first MESSENGER flyby for extrusive and explosive activity and the volcanic origin of the plains. *Earth and Planetary Science Letters* 285: 227–242.

Jagoutz E, Palme H, Baddenhausen H, et al. (1979) The abundance of major, minor and trace elements in the Earth's mantle as derived from primitive ultramafic nodules. In: *Proceedings of 9th Lunar and Planetary Science Conference*, pp. 2031–2050.

Jeanloz R, Mitchell DL, Sprague AL, and DePater I (1995) Evidence for a basalt-free surface on Mercury and implications for internal heat. *Science* 268: 1455–1457.

Keiffer WS and Murray BC (1987) The formation of Mercury's smooth plains. *Icarus* 72: 477–491.

Killen R, Cremonese G, Lammer H, et al. (2007) Processes that promote and deplete the exosphere of Mercury. *Space Science Reviews* 132: 433–509.

Killen RM and Ip W-H (1999) The surface-bounded atmospheres of Mercury and the Moon. *Reviews of Geophysics* 37: 361–406.

Krot AN, Meibom A, Russell SS, Alexander CMO'D, Jeffries TE, and Keil K (2001) A new astrophysical setting for chondrule formation. *Science* 291: 1776–1779.

Lawrence DJ, Feldman WC, Goldsten JO, et al. (2010) Identification and measurement of neutron-absorbing elements on Mercury's surface. *Icarus* 209: 195–209.

Lewis JS (1972) Metal/silicate fractionation in the solar system. *Earth and Planetary Science Letters* 15: 286–290.

Lewis JS (1974) Chemistry of the planets. *Annual Review of Physical Chemistry* 24: 339–351.

Lewis JS (1988) Origin and composition of Mercury. In: Vilas F, Chapman CR, and Matthews MS (eds.) *Mercury*, pp. 651–666. Tucson, AZ: University of Arizona Press.

Lodders K and Fegley B (1998) *The Planetary Scientist's Companion*. Oxford: Oxford University Press.

Lucey PG, Taylor GJ, and Malarete E (1995) Abundance and distribution of iron on the Moon. *Science* 268: 1150–1153.

Margot JL, Peale SJ, Jurgens RF, Slade MA, and Holin IV (2007) Large longitude libration of Mercury reveals a molten core. *Science* 316: 710–714.

McClintock WE, Bradley ET, Vervack RJ Jr., et al. (2008a) Mercury's exosphere: Observations during MESSENGER's first Mercury flyby. *Science* 321: 92–94.

McClintock WE, Izenberg NR, Holsclaw GM, et al. (2008b) Spectroscopic observations of Mercury's surface reflectance during MESSENGER's first Mercury flyby. *Science* 321: 62–65.

McClintock WE, Vervack RJ Jr., Bradley ET, et al. (2009) MESSENGER observations of Mercury's exosphere: Detection of magnesium and distribution of constituents. *Science* 324: 610–613.

McCoy TJ, Dickinson TL, and Lofgren GE (1999) Partial melting of the Indarch (EH4) meteorite: A textural, chemical, and phase relations view of melting and melt migration. *Meteoritics and Planetary Science* 34: 735–746.

McDonough WF and Sun S-S (1995) The composition of the Earth. *Chemical Geology* 120: 223–253.

Morgan JW and Anders E (1980) Chemical composition of Earth, Venus, and Mercury. In: *Proceedings of the National Academy of Sciences* 77: 6973–6977.

Murray BC (1975) The Mariner 10 pictures of Mercury. *Journal of Geophysical Research* 80: 2342–2344.

Murray BC, Strom RG, Trask NJ, and Gault DE (1975) Surface history of Mercury: Implications for terrestrial planets. *Journal of Geophysical Research* 80: 2508–2514.

Nittler LR, Starr RD, Weider SZ, et al. (2011) The major-element composition of Mercury's surface from MESSENGER X-ray spectrometry. *Science* 333: 1847–1850.

Peplowski PN, Evans LG, Hauck SA II, et al. (2011) Radioactive elements on Mercury's surface from MESSENGER: Implications for the planet's formation and evolution. *Science* 333: 1850–1852.

Potter A and Morgan TH (1985) Discovery of sodium in the atmosphere of Mercury. *Science* 229: 651–653.

Potter A and Morgan TH (1986) Potassium in the atmosphere of Mercury. *Icarus* 67: 336–340.

Prettyman TH, Hagerty JJ, Elphic RC, et al. (2006) Elemental composition of the lunar surface: Analysis of gamma ray spectroscopy data from Lunar Prospector. *Journal of Geophysical Research-Planets* 111: E12007 (41 pp).

Prockter LM, Ernst CM, Denevi BW, et al. (2010) Evidence for young volcanism on Mercury from the third MESSENGER flyby. *Science* 329: 668–671.

Rava B and Hapke B (1987) Analysis of the Mariner 10 color ratio map of Mercury. *Icarus* 71: 397–429.

Robinson MS and Lucey PG (1997) Recalibrated Mariner 10 color mosaics: Implications for Mercurian volcanism. *Science* 275: 197–200.

Robinson MS, Murchie SL, Blewett DT, et al. (2008) Reflectance and color variations on Mercury: Regolith processes and compositional heterogeneity. *Science* 321: 66–69.

Robinson MS and Taylor GJ (2001) Ferrous oxide in Mercury's crust and mantle. *Meteoritics and Planetary Science* 36: 841–847.

Scott ERD (1988) A new kind of primitive chondrite, Allan Hills 85085. *Earth and Planetary Science Letters* 91: 1–18.

Slade M, Butler B, and Muhleman D (1992) Mercury radar imaging: Evidence for polar ice. *Science* 258: 635–640.

Smith DE, Zuber MT, Phillips RJ, et al. (2012) Gravity field and internal structure of Mercury from MESSENGER. *Science* 336: 214–217.

Sprague AL, Hunten DM, and Lodders K (1995) Sulfur at Mercury, elemental at the poles and sulfides in the regolith. *Icarus* 118: 211–215.

Sprague AL, Kozlowski RWH, Witteborn FC, Cruikshank DP, and Wooden D (1994) Mercury: Evidence for anorthosite and basalt from mid-infrared (7.5–13.5 μm) spectroscopy. *Icarus* 109: 156–167.

Spudis PD and Guest JE (1988) Stratigraphy and geologic history of Mercury. In: Vilas F, Chapman CR, and Matthews MS (eds.) *Mercury*, pp. 118–164. Tucson, AZ: University of Arizona Press.

Strom RG (1977) Origin and relative age of lunar and mercurian intercrater plains. *Physics of the Earth and Planetary Interiors* 15: 156–172.

Taylor GJ, Boynton W, Brückner J, et al. (2006a) Bulk composition and early differentiation of Mars. *Journal of Geophysical Research (Planets)* 111: E03S10 (16 pp).

Taylor GJ and Scott ERD (2003) Mercury. In: Holland HD and Turekian KK (eds.) *Treatise on Geochemistry*, vol. 1, pp. 477–485. Oxford: Elsevier.

Taylor GJ, Stopar JD, Boynton WV, et al. (2006b) Variations in K/Th on Mars. *Journal of Geophysical Research (Planets)* 111: E03S06 (20 pp).

Taylor SR (1991) Accretion in the inner nebula: The relationship between terrestrial planetary compositions and meteorites. *Meteoritics* 26: 267–277.

Taylor SR and McLennan S (1985) *The Continental Crust: Its Composition and Evolution*. Oxford: Oxford University Press.

Vilas F (1988) Surface composition of Mercury from reflectance spectrophotometry. In: Vilas F, Chapman CR, and Matthews MS (eds.) *Mercury*, pp. 59–76. Tucson, AZ: University of Arizona Press.

Warrell J (2003) Properties of the Hermean regolith: III. Disk-resolved vis-NIR reflectance spectra and implications for the abundance of iron. *Icarus* 161: 199–222.

Wasson JT (1988) The building stones of the planets. In: Vilas F, Chapman CR, and Matthews MS (eds.) *Mercury*, pp. 622–650. Tucson, AZ: University of Arizona Press.

Weidenschilling SJ (1976) Accretion of the terrestrial planets II. *Icarus* 27: 161–170.

Weisberg MK, Prinz M, Clayton RN, and Mayeda TK (1993) The CR (Renazzo-type) carbonaceous chondrite group and its implications. *Geochimica et Cosmochimica Acta* 57: 1567–1586.

Weisberg MK, Prinz M, Clayton RN, Mayeda TK, Grady MM, and Pillinger CT (1995) The CR chondrite clan. In: *Proceedings of NIPR Symposium on Antarctic Meteorites* 8: 11–32.

Wetherill GW (1988) Accumulation of Mercury from planetesimals. In: Vilas F, Chapman CR, and Matthews MS (eds.) *Mercury,* pp. 670–691. Tucson, AZ: University of Arizona Press.

Wetherill GW (1994) Provenance of the terrestrial planets. *Geochimica et Cosmochimica Acta* 58: 4513–4520.

Zurbruchen TH, Raines JM, Gloeckler G, et al. (2008) MESSENGER observations of the composition of Mercury's ionized exosphere and plasma environment. *Science* 321: 90–92.